



Drawing down the remaining copper inventory in a leach pad by way of subsurface leaching



Dale F. Rucker^{a,*}, Robert J. Zaebst^b, Jim Gillis^c, Joseph C. Cain IV^a, Bruce Teague^b

^a hydroGEOPHYSICS, Inc., Tucson, AZ, USA

^b Carlota Copper Company, Miami, AZ, 85539, USA

^c Metallurgical Consultant, Miami, AZ, 85539, USA

ARTICLE INFO

Article history:

Received 20 September 2016

Received in revised form 23 February 2017

Accepted 27 February 2017

Available online 2 March 2017

Keywords:

Copper

Leach

Inventory

Modeling

Monitoring

ABSTRACT

A significant amount of metal inventory can reside in a leach pad due to unfavorable metallurgical and hydraulic conditions. Continued leaching using surface irrigation will likely be unsuccessful at recovery in any reasonable time frame. In this work, we investigate how subsurface leaching (SSL), using wells to facilitate the delivery of barren solution, could potentially increase recovery and drawdown the inventory in a shorter period of time. An initial characterization campaign of the leach pad using drilling and assaying along with geophysical methods showed that inventory was high because the ore remained dry from compaction. Other areas were also shown to have preferential flow paths as a means to drain solution out of the leach pad. Assaying results taken from sonic coring and auger cuttings, and extrapolated across the leach pad, revealed a potential of 37×10^6 kg of acid soluble copper.

Our investigation covers the first 1000 days of SSL, with 110 PVC wells distributed across five main areas. During this time, we estimate production at 2.26×10^6 kg of copper based on the amount of solution introduced through the wells multiplied by the average copper grade from a number of sources, including monitoring wells and newly formed side slope seeps. Some areas performed better than others, especially where assays revealed that acid soluble copper was greater than 50% of total copper. The SSL program is expected to continue for at least another 1000 days, and we expect an additional 7×10^6 to 15×10^6 kg will be withdrawn from inventory.

© 2017 Elsevier B.V. All rights reserved.

1. Introduction

Low hydraulic conductivity within heap leach pads can cause difficulty for extraction of metal through a surface leach operation. For a homogeneous ore with uniform hydraulic properties, a significant amount of time is needed for the lixiviant to percolate through the pile. Studies have shown, however, that the lixiviant typically does not percolate uniformly through the ore (e.g., Rucker, 2010) and will find ways to preferentially flow along localized structural components with higher conductivity (Wu et al., 2006; McBride et al., 2012). On the surface, this may be evidenced by local ponding adjacent to well drained ore. Conditions that may contribute to preferential flow include irrigation rates near the saturated hydraulic conductivity (Seyfried and Rao, 1987), restrictive layers - inclined or otherwise (Allaire et al., 2009), the existence of macropores (Jarvis et al., 1999), and flow instability generated from stacking a finely crushed ore atop a coarser ore (Rezanezhad et al., 2006). When non-uniform percolation does occur, a significant reserve of metal will remain in the pad's inventory due to large volumes of underleached ore.

Increasing the metal recovery from low permeability heaps has been the focus of many published studies; these studies span the design, operational, and post-operational periods. At the design phase, investigations have been motivated to understand parameters that are easily controllable, such as heap height (Mellado et al., 2011; Trujillo et al., 2014), irrigation rate (Saririchi et al., 2012; Silver, 2013; Rucker et al., 2015), aeration (Mahmoudian et al., 2014), or a combination of these factors (Lizama et al., 2005). During the operations phase, details affixed to agglomeration (e.g., Bouffard, 2008) are an obvious choice for study and fine-tuning since environmental and geometallurgical conditions can change daily or seasonally. At the post-operational phase and prior to closure, rinsing with fresh water has been studied as a means to reach interstitial porewater that has been trapped in dead end pores (Catalan and Li, 2000; Howell et al., 2009). Hydrogeologically speaking, the fresh water has a lower viscosity than the lixiviant and dilution will allow flow through otherwise immobile regions. In more recent years, subsurface leaching (SSL) has been gaining attention as a post-operational phase enhancement (Ghorbani et al., 2016) and it is this method which will be discussed in detail.

To date, much of the study and application of SSL methods has been within gold leach operations (e.g., Rucker et al., 2009; Seal et

* Corresponding author.

E-mail address: drucker@hgiworld.com (D.F. Rucker).

al., 2012; Winterton and Rucker, 2013; Rucker et al., 2014). The general concept behind SSL is to direct the barren solution to areas deep within the leach pad in order to 1) target those areas that have been traditionally underleached, and 2) reduce the drainage time of pregnant leach solution out of the pad. The concept of SSL is similar to in-situ leaching of ore bodies (e.g., Sinclair and Thompson, 2015). The directed solution is facilitated through a well that is screened over one or more intervals. If the pressures of the SSL are significantly high, the process may create a new set of drainage channels that will further enhance surface leaching.

A pilot study of SSL in a copper heap showed success for delivering lixiviant to underleached material in the deeper reaches of the pile. Over the operational period of the mine, surface geophysics had been conducted to map the locations of these underleached areas (Cubbage et al., 2016), which helped to site the wells for the pilot study. The SSL test was also shown to increase copper concentration in the pregnant leach solution (PLS). Under highly controlled experimentation, Rucker (2015) showed that compacted, low permeability ore developed from truck dumping can easily accept 90 m³/h and up to 200 m³/h, at top-hole pressures less than 0.2 MPa. It is hypothesized that the fine grained material became fluidized and moved out of the immediate vicinity of the wellbore, thus leaving behind larger particles accompanied by large open pore spaces. Furthermore, copper was shown to be upwards of 3.8 g/L for a short period of time, with sustained values of 1.5 g/L compared to 1 g/L from nearby drains intercepting surface-leached PLS. In this paper, we extend the work from the pilot study by Rucker (2015) to show how engineering parameters developed from the test were upscaled to cover a large portion of the leach pad. Additional adjustments to flow rate and timing of injections were made to accommodate ore with secondary sulfides. Lastly, a resource extraction model was developed to show the trajectory of copper recovery in preparation for closure.

2. Site and ore description

The SSL project was conducted at the Carlota Mine, located within the Globe-Miami mining district of central Arizona. The mine is an open-pit comprising two nearby deposits that include the Carlota and Cactus; these deposits straddle the Pinto Creek with the Cactus on the east side and Carlota on the west side. The two deposits are hosted in a landslide breccia of Pinal schist (Peterson, 1962; Cook, 1994), with a southern bounding fault of brecciated diabase. The deposit is overlain by Apache Leap volcanics, such as dacite and tuff.

Copper mineralization mainly occurs in the breccia, the overlying dacite, and along the clay-rich southern bounding fault. Chrysocolla is persistent across the site, with malachite found locally abundant in the eastern portion of the Cactus deposit and sporadically along the fault. Chalcocite is the only significant copper sulfide mineral present and is restricted to the lower parts of the deposits. Chalcocite is commonly found rimming or partially to totally replacing pyrite, which is often found as veinlets or individual grains within brecciated clasts. Secondary sulfide mineralization is generally quite uniform and consistent, often grading about 0.70% copper. The oxide ore is more erratic in distribution and grade.

A single valley fill heap, divided into two phases, is created from a run-of-mine process through blasting, loading, and truck haulage of ore, followed by SX/EW processing to produce cathode copper. The ore has high levels of fines in the ore matrix and relatively low compressive strength in-situ. The friable character of the ore has resulted in reduced percolation rates. Midway through the heap creation, however, operations switched from truck dumping to retreat conveyed stacking. Another change to improve percolation through the upper material was pre-wetting the ore prior to stacking, which increases the hydraulic conductivity of the material.

3. Heap characterization

Slow percolation was observed early in the heap's creation and much effort was expended in characterizing the degree of nonuniformity in lixiviant coverage. The main characterization methods included 1) drilling accompanied by assaying for metal content and moisture and 2) electrical resistivity imaging. Drilling was mostly conducted by sonic to allow for intact cores. Electrical resistivity was conducted along the surface using the Schlumberger array (Loke et al., 2013; Rucker and Glaser, 2015) to observe broad distributions of the electrical structure as it relates to pertinent hydraulic and metallurgical phenomena. Equipment and procedures for data acquisition and modeling were conducted similar to that described in Chávez et al. (2015), Dunbar et al. (2015), and Swarzenski et al. (2016). Fig. 1 shows the locations of the characterization effort across the leach pad. These data can be separated into characterization conducted before and after any SSL project commenced.

3.1. Pre SSL

The initial electrical resistivity was collected in 2009 and spanned large areas of the Phase 1 leach pad. The purpose of the survey was to help pinpoint areas within the heap that were causing ponding. Fig. 2 shows the results of the survey as contours of electrical resistivity along each of the two profiles. The depth of investigation for the survey extended to the HDPE liner, which is draped over the valley hosting the leach pad. Low values of resistivity are usually associated with moist material, porewater of high ionic strength, or clayey ore.

Profile A-A' shows a wide range of resistivity, spanning nearly four orders of magnitude. The beginning of the profile exhibits lower resistivity values, especially at the surface where fresh ore under leach is highly saturated and of high acid strength. The center of the profile shows relative homogeneity. The end of the profile is much more resistive as new ore was just placed and was not under leach. Profile B-B' reveals ore that is significantly drier, with what appears to be preferential flow channels located at 150 m, 450 m, and 575 m. The channels manifest as vertically elongated stripes of very low electrical resistivity.

Sonic drilling occurred sporadically before SSL and did not coincide directly with the timing of electrical resistivity acquisition. Fig. 3A and B shows examples of drilling results, taken from locations that were in close proximity to Profile A-A'; their locations are extrapolated to respective positions in Fig. 2. LPD-22 and LPD-23 were drilled in 2010, after the resistivity was acquired and additional ore was stacked. The moisture data is uniform along the profiles, similar to the electrical resistivity data at that location. Total copper is more variable, but the trends between the drill holes are the same. Furthermore, there is an indirect correlation between the trends of moisture and trends in total copper. That is, when moisture increases the copper decreases, which suggests that if the ore is sufficiently wetted then copper leaching will occur.

The second pair of sonic data occurred in the area of the resistivity profile that was more heterogeneous in nature. LPD-37 shows the same indirect correlation between moisture and total copper and a very wet zone at a depth of 1177 m is almost depleted of copper. Curiously, the trends in total copper from LPD-37 and LPD-38 are opposite but moisture trends are similar, save the one extreme point in LPD-37. Overall, it appears that the electrical resistivity can describe trends in moisture but there is no correlation with total copper.

3.2. Post SSL

After the SSL program started, periodic electrical resistivity profiles were taken before drilling commenced for each new well field. Profile C-C' (Fig. 4) was acquired in 2015 to understand the effects of previously injecting at the north end of the profile (near well cluster Group α) and to gain an appreciation of the resource in the center of the profile (near Group β). Overlain on the profile is a dashed line demarcating

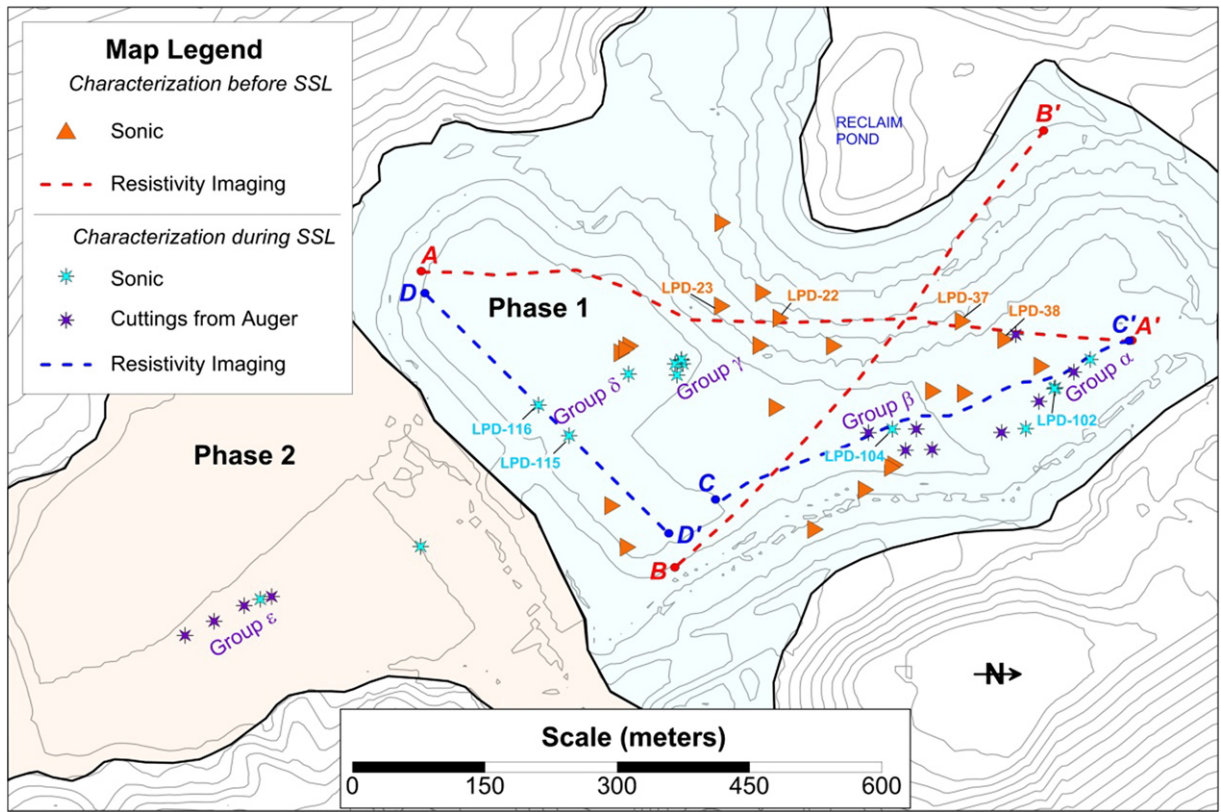


Fig. 1. The heap leach pad at the Carlota Mine with characterization before and after SSL commenced. Characterization was limited to drilling and electrical resistivity geophysics with individual resistivity lines and leach pad drill holes (LPD) identified.

the elevation of the heap during the 2009 electrical resistivity and the positions of two sonic wells taken at the time of the survey. The resistivity data show a low conductivity layer persistent across the line, around

elevation 1200 m. Moisture data for LPD-102 and LPD-104 (Fig. 3C) show elevated saturation coincident with this depth, along with depleted copper. The material at the bottom of the profile is more resistive

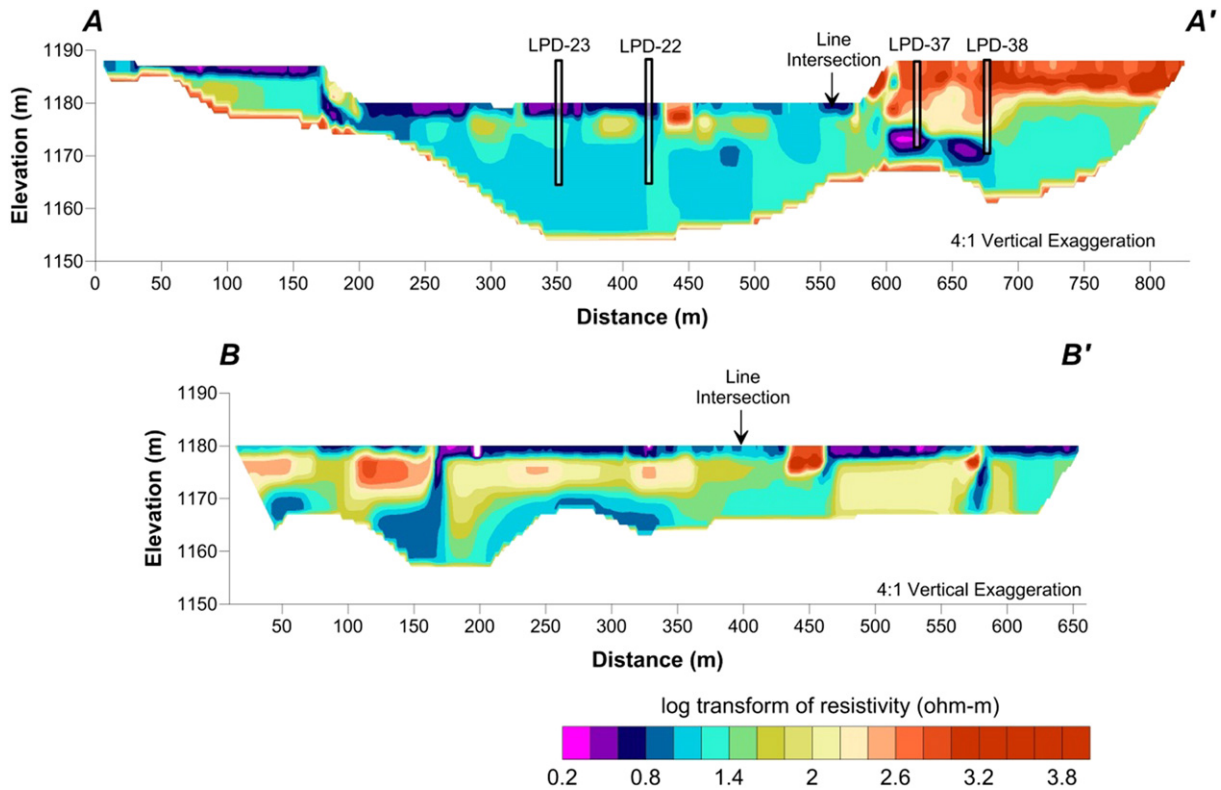


Fig. 2. Pre SSL electrical resistivity characterization.

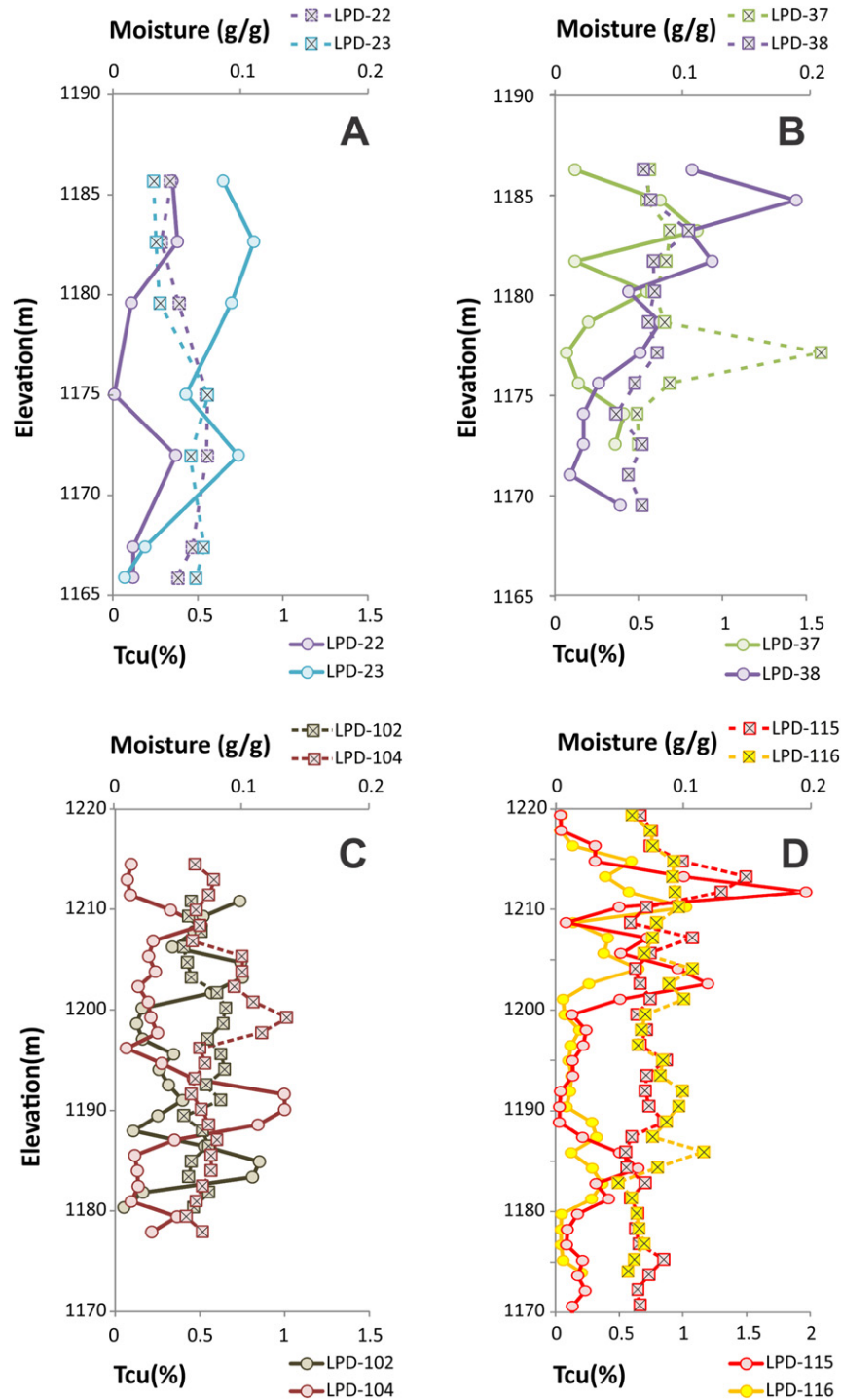


Fig. 3. Sonic drilling and assay for boreholes located in close proximity to electrical resistivity profiles, showing mass-based moisture and total copper (Tcu). A) assay results in the center of Profile A-A', B) assay results near the end of Profile A-A', C) assay results along Profile C-C', and D) assay results along Profile D-D'.

than material above it, but uniform compared to data acquired in 2009. It is hypothesized that over the six years, some lixiviant was able to percolate into the lower reaches of the truck-dumped ore, but likely not at a rate that would suggest adequate drainage.

Most recently, electrical resistivity Profile D-D' (Fig. 4) was acquired to understand conditions prior to drilling a new well field, along with three sonic holes (Group δ in Fig. 1). The resistivity profile shows much more uniform electrical properties compared to profile C-C'. In this area, however, the remaining copper was directly correlated with moisture (Fig. 3D). Given the combination of high copper, high moisture, and uniform electrical properties, it is likely that the ore is of

lower hydraulic conductivity with very slow drainage. Solution samples taken from LPD-116 showed copper in excess of 1 g/L and a pH greater than 2.5. The area, therefore, is prime for SSL to enhance recovery of the copper.

3.3. Resource model

From the assay data, a resource model was created for the heap to calculate the remaining copper after surface irrigation had ceased. The Phase 1 heap was distributed into four groups (Fig. 1), each with a set of assay data and a center of mass. Each group's center of mass was

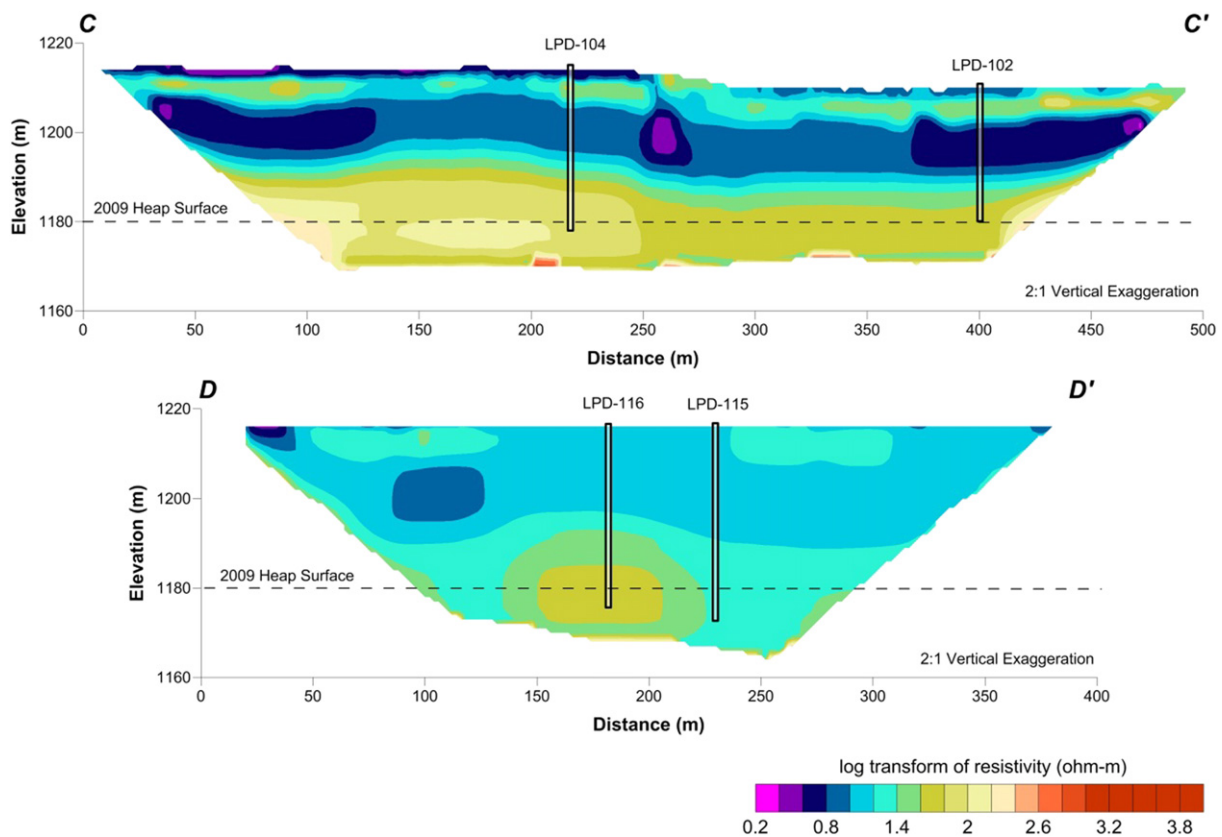


Fig. 4. Post SSL electrical resistivity characterization, with profile C-C' acquired in 2015 and profile D-D' acquired in 2016.

then used to divide the heap according to a nearest neighbor geostatistical routine. Phase 2 comprised of a single group. Table 1 lists the volume occupied by each group, calculated simply by subtracting the elevation of the liner from the elevation of the top surface along discrete points with a fixed area of 10m². The deepest part of the pad was approximately 67 m, which thinned to zero at the edge of the liner.

To obtain the total copper, heap density and copper grade were needed from the drilling data. Sonic drilling provided information with regards to density. From 155 core samples, the average density was approximately 1.46 g/cm³ with a standard deviation of 0.25 g/cm³. These data were used to calculate heap mass, which summed to 28 million Mt. Samples from both sonic cores and cuttings from auger drilling were assayed for total copper and an acid soluble copper value using a 24-hour bottle roll test. The copper grade statistics in Table 1 were generated from a total of 525 samples. The data show that all five areas of the pad have a similar grade of total copper, with Group α having a slightly larger total grade, but with the least soluble in acid. Group γ has a solubility nearly double that of α , which is directly reflective of the amount of sulfidic ore in each area.

Table 1

Resource model data to estimate the remaining copper in inventory for the Phase 1 leach pad.

Phase	Group	Heap volume (m ³)	Heap mass (Mt)	Average total Cu (%)	Average acid soluble Cu (%)	Total Cu mass (kg)	Acid soluble Cu mass (kg)
1	α	2.6×10^6	3.8×10^6	0.37	0.09	14×10^6	3.5×10^6
1	β	2.5×10^6	3.7×10^6	0.30	0.11	11×10^6	4.1×10^6
1	γ	4.4×10^6	6.5×10^6	0.33	0.17	22×10^6	11×10^6
1	δ	4.8×10^6	7.0×10^6	0.31	0.16	21×10^6	11×10^6
2	ϵ	4.6×10^6	6.7×10^6	0.29	0.11	19×10^6	7.6×10^6
Total		19×10^6	28×10^6			87×10^6	37×10^6

Lastly, the copper grades were multiplied by the heap mass to get an estimate of the total copper and acid soluble copper mass in the pad's inventory. The data reveal a significant reserve of metal, with 37,000,000 kg that could be leached, provided that acid reaches the ore and can drain to the liner. Fortunately, secondary recovery provides the mechanism for both, by directing the acid to specific underleached regions and increasing the hydraulic driving force to ensure that drainage occurs.

4. Subsurface leaching

Using the results from the pilot test (Rucker, 2015), engineering parameters were developed for an upscaled well design to cover the rest of the heap. Specifically, the multi-well SSL test from the pilot test, using four simultaneous injection wells, appeared to distribute the solution over the broadest area with rates that could easily exceed 340 m³/h. Fig. 5 shows the well layout across the leach pad to date, with a strategy of discrete SSL areas operating for a period of time. Monitoring wells accompany injection wells to extract samples for metallurgical analysis, track the drawdown of inventory in the pad, and to ensure phreatic conditions are at a safe level.

The first SSL area after the pilot test was located at the north end of the leach pad, near Group α . Four pods of five to six wells per pod were installed within the 4.3 ha area, with the wells placed significantly far from the edge to minimize risk from a saturated slope failure. To further mitigate risk, a monitoring well was placed near the side slope to monitor specifically for the phreatic level. Its location was chosen based on the drainage pattern offered by the topography of native ground. The bottom of the monitoring well was 6 m above the liner. During the entire SSL period to date, the well has remained dry.

Metallurgically, this area proved to be difficult to leach due to the higher percentage of sulfide copper, likely in the form similar to covellite, and low acid soluble oxide copper in the ore (Table 1). However,

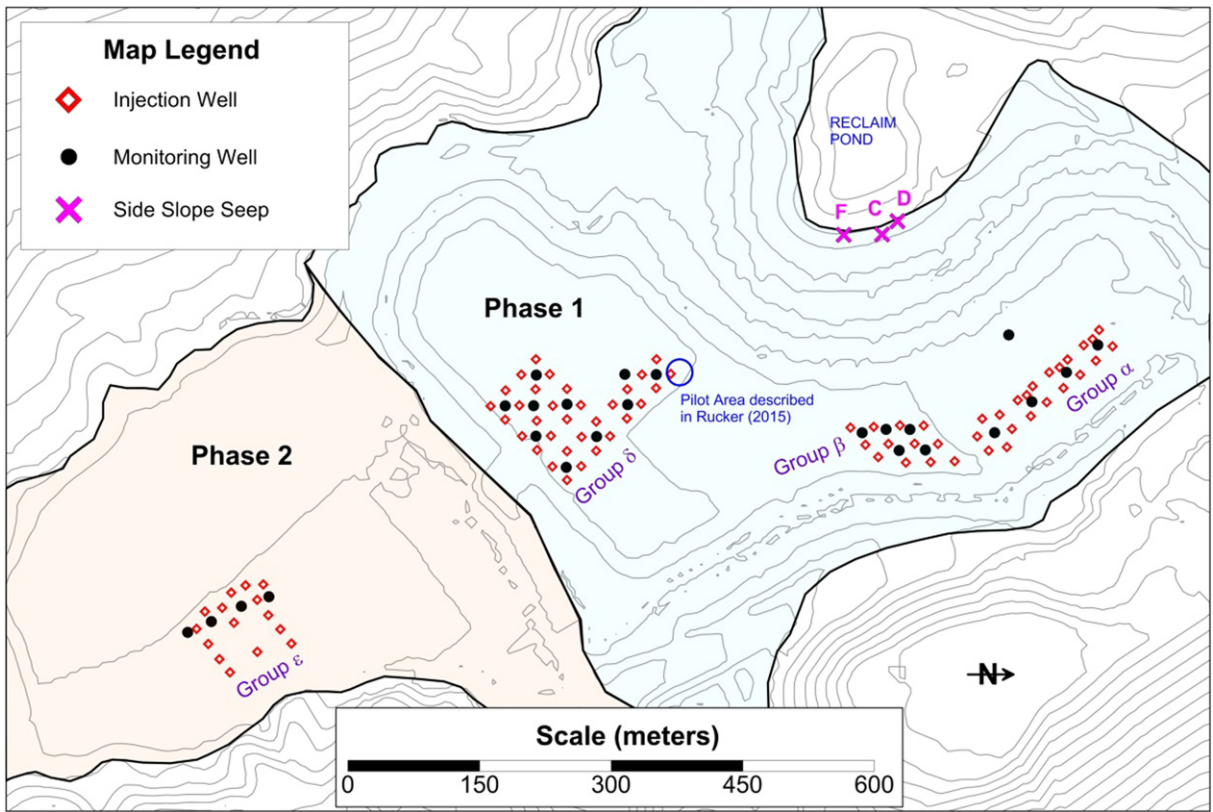


Fig. 5. SSL well distribution across the heap leach pad.

no mineralogy of the ore samples was conducted to verify the copper-sulfur assemblages. Solution samples from monitoring wells showed low copper concentration in the PLS soon after SSL started. Fig. 6

shows PLS and raffinate copper grades for the first 50 days of SSL, including an example from Group α (Fig. 6A) and from the oxide-rich pilot test area (Fig. 6B). Whereas the copper grade in the PLS during

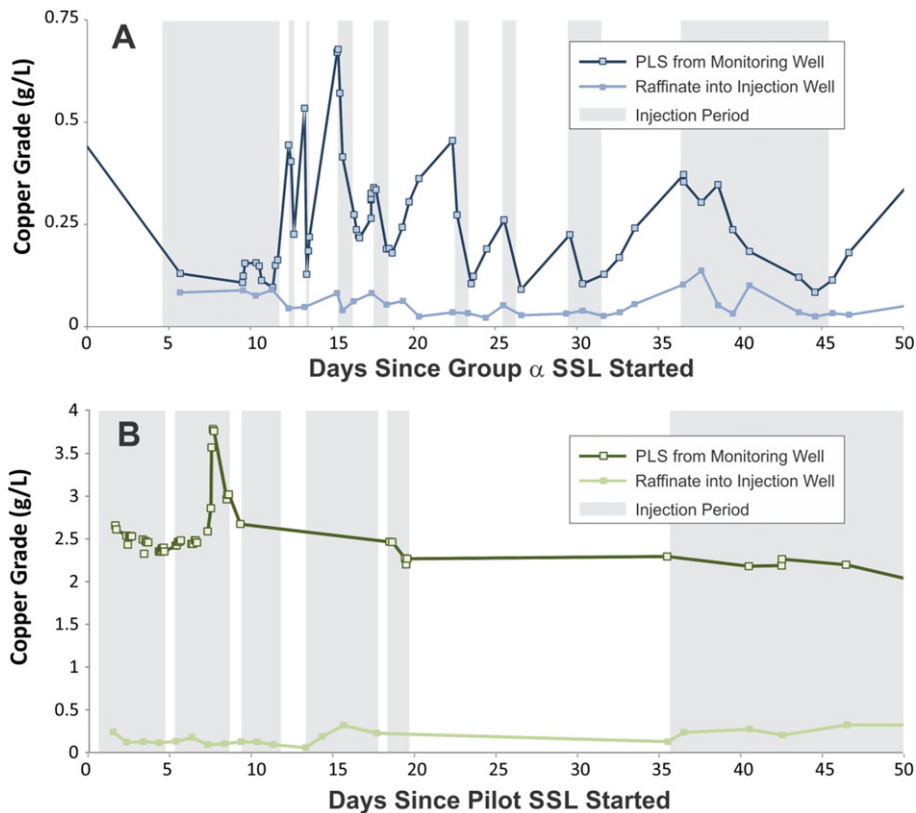


Fig. 6. Time series of copper grades from PLS extracted from monitoring wells and raffinate used in SSL. A) Data from wells near Group α; B) Pilot test results (adapted from Rucker, 2015).

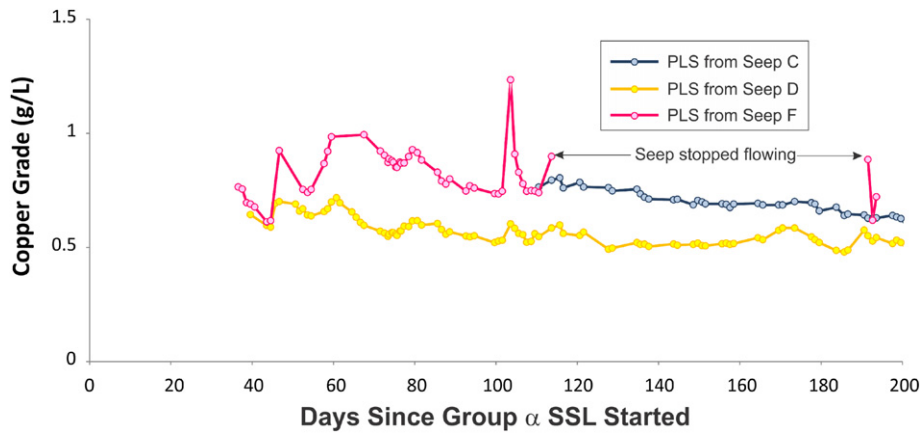


Fig. 7. Copper grade in PLS from several side slopes seeps.

the pilot test remained high regardless of injection timing, the grade in the sulfide rich area diluted quickly but recovered when SSL was turned off. That is, the ore benefited from a resting period to accommodate the slow kinetics of leaching the sulfide ore.

During the course of the injection period, several low-flow seeps formed on the side slopes below the injection area. The flow rates were on the order of 1–2 L/min. The seeps were re-invigorated during SSL after initially forming from surface leaching, but were dry before SSL. The seeps provided a means for additional metallurgical sampling locations and Fig. 7 shows the copper grade from three seeps that were in close proximity to each other and along the same stratigraphic horizon (Fig. 5). The first of these seeps appeared 36 days after SSL began on Group α; a few others (not shown) formed a week or two earlier. The data from these seeps show a range of responses. Seep F, for example, had significantly better grade than Seep D, but was less consistent in flow. It is hypothesized that Seep F stopped flowing for a period due to a specific arrangement of wells receiving raffinate. Seep C appeared much later than D or F and fits within the paradigm of copper grades from F. Additionally, they all have a gradual and steady decrease in grade over time. Overall, it is clear that the seeps are from isolated preferential flow paths within the lower portions of the pad based on their unique values. It also shows that once the raffinate had a chance to percolate through larger volumes of ore, that more copper is dissolved than suggested solely by the monitoring wells. The seeps likely give a better accounting of copper extracted than the monitoring wells.

Due to the difficult drainage conditions in the heap, local perched aquifers have developed. The perched aquifers are mainly above the interface between the more permeable retreat stacked ore and the compacted truck dumped ore. These aquifers appear compartmentalized in that they are at different elevations and discontinuous across

the pad. For example, Fig. 8 shows the response of water levels to SSL in the Group β area. The five monitoring wells represent an area of about 1 ha and show a range of water levels spanning approximately 26 m before SSL started. Additionally, the levels in MT5, 6, and 8 were virtually identical. After SSL, the water levels from each pod had a different response depending on location. Monitoring wells MT5 and MT7 on the east side of the well field showed little to no change, while the levels in the remaining wells were highly variable. The rise and fall of water levels around the area can be related to timing of raffinate applied to specific wells and almost all wells return to their respective original water level once SSL is turned off.

At first glance, the increase in water levels appears to approach dangerous levels. Well MT6 rose 10 m in a short period of time and drained slowly. To put these water level data in context, electrical resistivity monitoring was conducted for the first seven days of SSL to observe how the solution propagated outward and whether the PLS was draining effectively to the liner. Resistivity data were collected every 20 min using a combination of electrodes on the surface and on the outside casing of monitoring wells. Fig. 9 shows a snapshot taken on the last day of monitoring. The data represent a three dimensional rendered body of electrical resistivity values that have decreased 15% or more compared to a background resistivity dataset collected prior to SSL. A description of electrical resistivity and data presentation can be found in Rucker (2010, 2015). The results of the resistivity monitoring are confirmed by the water level data (Fig. 8) in that all of the changes in water levels are observed in well MT6, 8, and 9. Furthermore, the solution build up is isolated to be near the well field and has reached the liner. The solution is draining along the deepest portion of the liner (indicated as a color contoured surface in Fig. 9) towards the reclaim pond. In all of the resistivity monitoring of SSL at Carlota, drainage has always occurred along the topographical gradient of the liner.

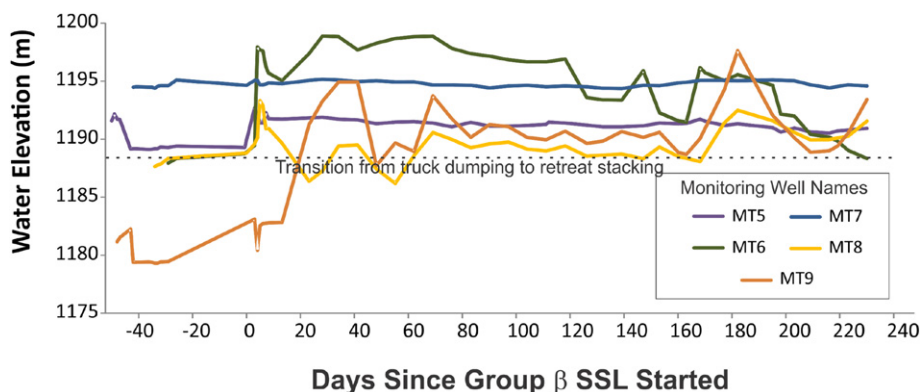


Fig. 8. Water levels in the leach pad as measured from monitoring wells in Group β. Negative days since SSL started are reflective of the drilling and well development period.

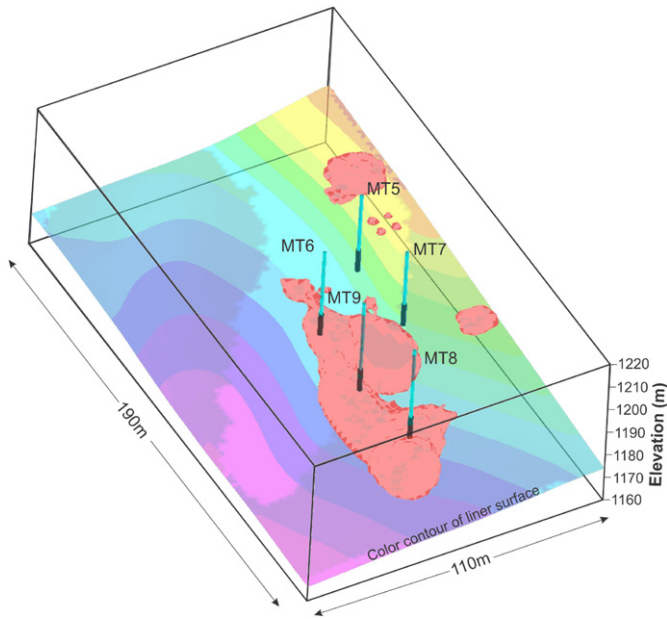


Fig. 9. Electrical resistivity data showing coverage of solution (combination of raffinate and PLS) during SSL. The data were taken seven days after SSL started in Group β. The solid body rendering represents a decrease in resistivity of at least 15% compared to background conditions prior to SSL. MT wells are monitoring wells to capture solution for metallurgical analysis.

5. Extraction model

A financial model, based on the mass of copper liberated, is needed to justify use of the SSL method. In Rucker (2015), the average net copper grade (in mass per volume) from each well was multiplied by the volume of injected raffinate to calculate the final mass of copper. The net copper was considered by subtracting the average raffinate copper grade from the in-situ copper grade. Furthermore, the calculations were divided between the initial short term pulsed rinse phase and the longer continuous rinse phase, whereby it was estimated that 0.19×10^6 kg of copper was liberated in 96 days.

For the continuation of the SSL program across the entire heap, flow meters at each well head are used to accurately account for the raffinate input. The raffinate generally had 3 g/L of free acid and an average 0.13 g/L copper. Fig. 10A shows the total SSL flow volume to each of the grouped areas, including the initial pilot scale test (as Group γ). Summing the flow from each area, the total injected volume by day 1000 was 5.17×10^6 m³ (or 1.37 billion gallons). The area with the most total flow was Group α, which has had a reduced flow for the last year due to declining grades. Group ε has been shut off for some time, also due to very low recoveries.

The concentration of copper and other metallurgical parameters were tracked by extracting solution samples from monitoring wells in the immediate vicinity of the injection wells and from low flow seeps on the side slopes. The data from many of these sources were used to establish an average grade representative of SSL copper liberation. Fig. 11 shows data from four areas within the Phase I leach pad with their

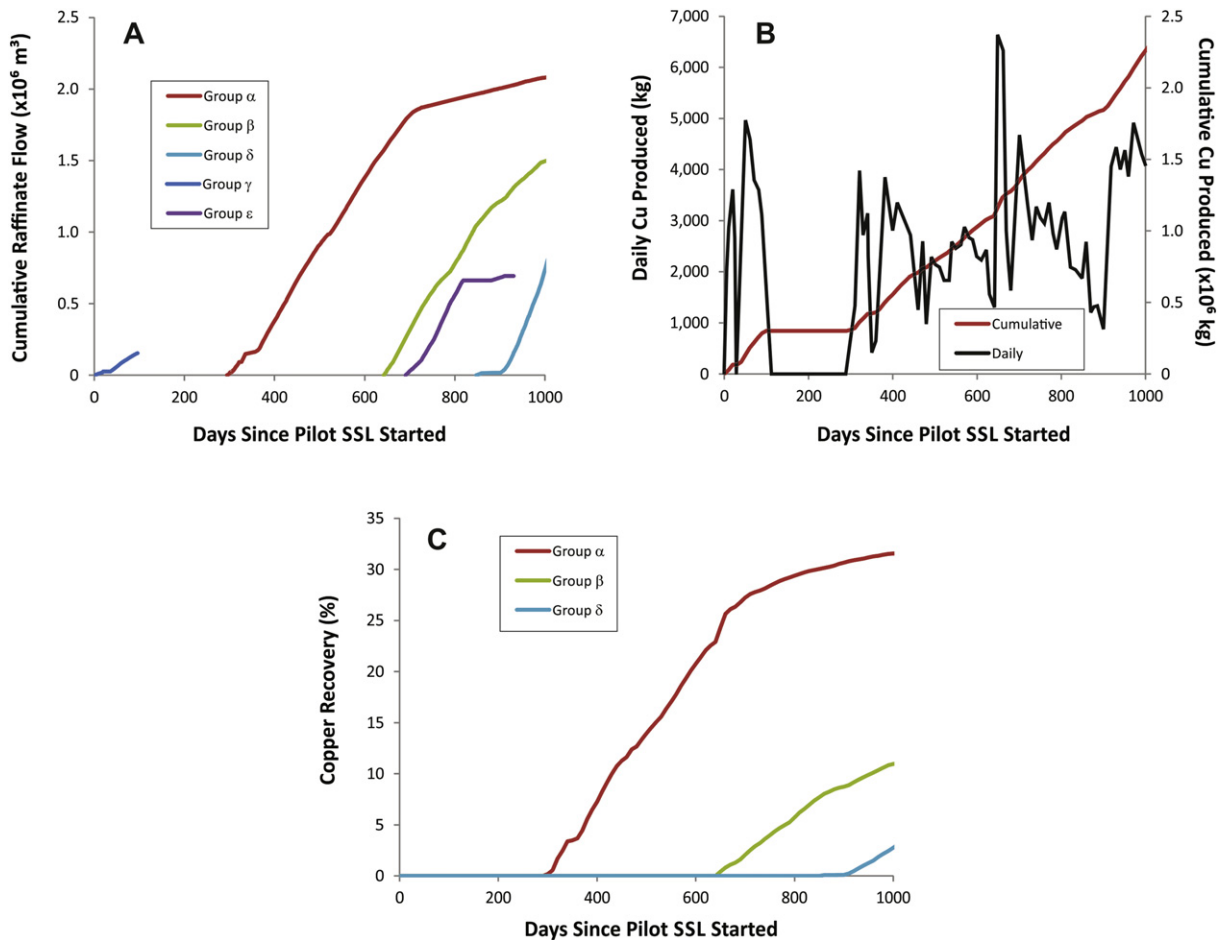


Fig. 10. A) Cumulative flow of raffinate to each of the well groups. B) Cumulative and daily copper production from all groups combined. C) Percentage of copper recovery from groups within the Phase I leach pad.

sources used in determining average grade. The goal was to use six sources for establishing the representative grade, which were from a mixture of monitoring wells and seeps. The exception to this was the pilot test, which had only four sources available for the entire duration of the 95 day test. The sources for all areas were unique and identified generically as Sources 1 through 6 in the figure. Generally, the copper grades were within the range of 0.5 to 1.5 g/L. All of the sources also show a general decreasing trend of copper grade over time, but remain well above the input copper grade offered by the raffinate. Small, temporal-scale variability is also observed, where spikes of high and low copper grade can be related to individual injection events within a group of wells. For example, as new wells are turned on in a group,

there will a slight increase in grade. As the grade falls over time, different wells will take turns at injection to maintain a higher grade over the long term. Thus, active management of the SSL program is used to ensure an optimum production.

The results of total copper production are shown in Fig. 10B, which shows the daily copper and cumulative copper over the 1000 day project. Again, the average copper grade from each group (less the copper grade within the raffinate) was multiplied by the volume of raffinate introduced to the heap to obtain the mass of liberated copper. The daily copper production shows periods of rapid increase that are correlated to times of bringing on a new well field for SSL. The highest sustained daily production occurs in Groups δ and γ , which are near each other

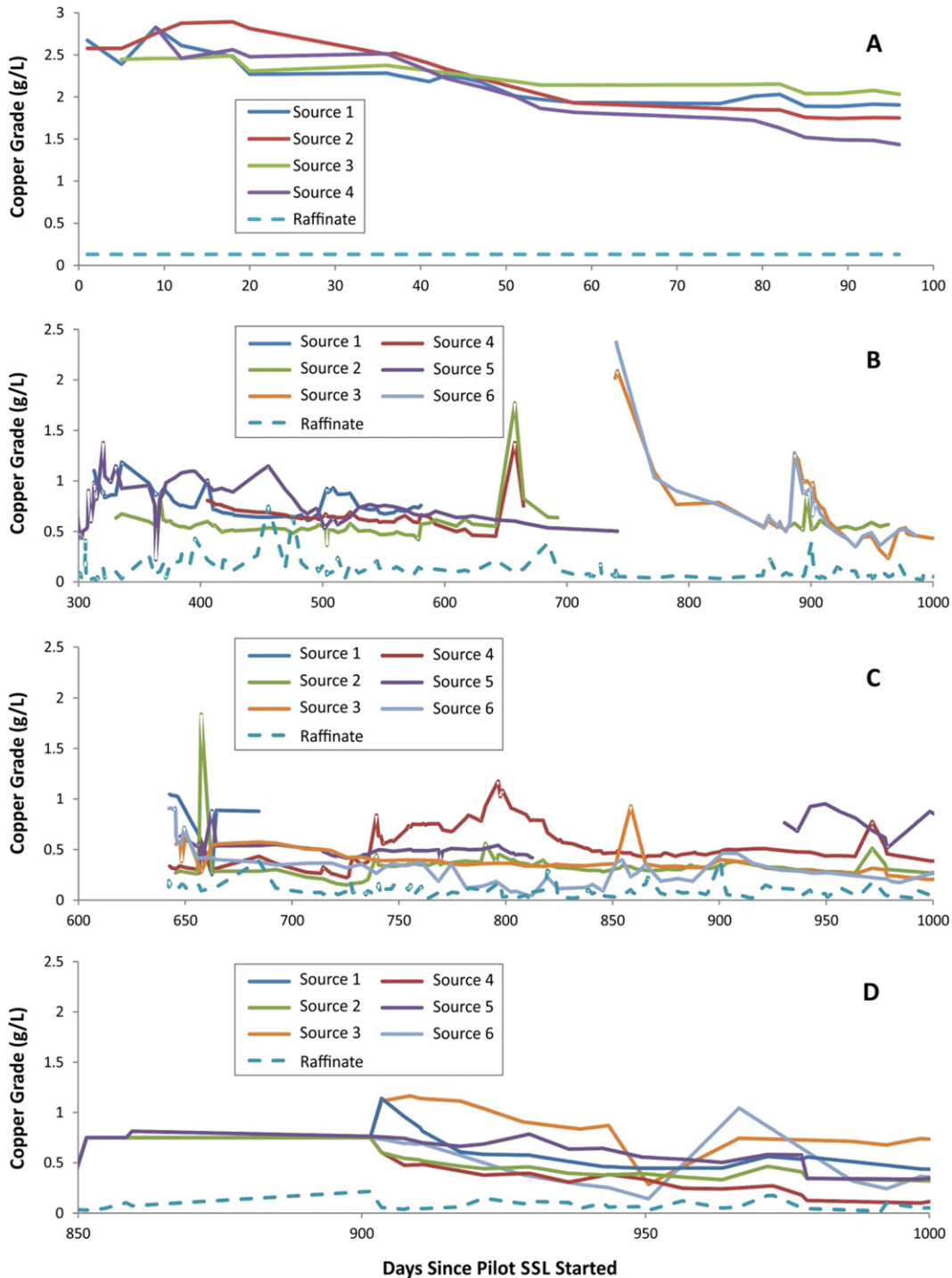


Fig. 11. Copper grades from different sources near injection wells for the different SSL areas of the Phase I leach pad: A) the pilot scale area, Group γ , B) Group α , C) Group β , and D) Group δ .

in the center of the Phase I leach pad. However, this is a spike of production that occurs around day 650, approximately one week after Group β started. Several sources showed a high copper grade for a brief period of time, which contributed to the increase in mass for that area. From a cumulative perspective, we estimate that a total of 2.26×10^6 kg of copper has been liberated, which is 6.1% of the acid leachable inventory and 2.6% of the total copper inventory.

Finally, Fig. 10C shows the copper recovery for the three main areas of the Phase I leach pad. The data for the Phase II leach pad (coinciding with Group ϵ) is not shown, because little production has been seen from that area. The recovery percentage was calculated by dividing the cumulative copper production from each area by the available acid soluble copper of Table 1. The figure shows that a substantial portion of copper has been extracted from Group α , but the production rate has tailed off over time due to low injection volumes and low grades. To extract the next 30%, it is likely that more wells will be needed to the west of the current set of wells. The trajectory of recovery for Groups β and δ looks similar, but only because the amount of copper to extract from Group δ is much higher (4.1 vs 11×10^6 kg). The rate of copper production from Group δ is significant and we expect another 1.1×10^6 kg of copper to be extracted from that area in the next year, if the rate holds. This is compared to the extraction of 0.09×10^6 kg from Group β for the same period.

The resource recovery model presented for the SSL program is difficult to verify by other means. Hypothetically, verification could come from using the flow rates and copper grades in the reclaim pond to calculate the total copper produced, similar to the work in Seal et al. (2012) for the CC&V project. The proportion of flow to either surface or subsurface flow is always known and varies between a split of 90–10 and 60–40, with the higher percentage to surface leaching. The unknowns are the copper grades that represent either surface leach or SSL. This puts us in a condition of having two unknowns with only one equation and a large number of possible solutions (barring those that are physically impossible). Again, Seal et al. (2012) assumed a base grade from surface leaching, but that value could not be validated. Another means of verification of our SSL could be to sample the heap internally to calculate the drawdown of copper reserves. Assays of ore taken before and after SSL could be used in a mass balance approach to compare to the extracted amount. Rucker (2015) qualitatively compared these types of data for samples near an injection well and showed drawdown of total copper below the injection zone. Perhaps the internal sampling approach is how we will validate SSL in the future, but we don't have enough cores as of yet to conduct this type of analysis.

6. Conclusions

An SSL program is underway at the Carlota mine. The program has been in operation for about 1000 days, beginning with a pilot scale test. The pilot scale test was conducted to develop engineering parameters in order to upscale a well field across both leach pads on the mine. These parameters included a generalized well spacing, duration of injection, and a flow rate to the well that can accommodate drainage. Additionally, models were developed to estimate inventory drawdown.

Now, under full operations, some methodologies have been amended to allow for different metallurgical and hydraulic properties than were encountered in the pilot scale test areas. Sulfide-rich ore, for example, has slower kinetics for copper liberation and the injection timing was altered so that the pregnant leach solution was not overly dilute. Characterization and monitoring of the SSL program has been key to making these adjustments as well as developing realistic inventory extraction models. Over time, the models have become more conservative to account for a range of unknown conditions encountered in the leach pad.

The SSL program is expected to run at least another 1000 days. In that time, we expect a range of 7 to 15×10^6 kg of copper to be liberated, depending on the percentage of flow dedicated to the wells; currently

about 40% of the flow is directed to SSL and the remaining is used for surface leaching. The drawdown will also be accomplished by investing in more wells across both phases of the leach pad and continued optimization of well designs, injection timing, and potentially some level of automation in monitoring and flow control.

Appendix A. Supplementary data

Supplementary data to this article can be found online at <http://dx.doi.org/10.1016/j.hydromet.2017.02.024>.

References

- Allaire, S.E., Roulter, S., Cessna, A.J., 2009. Quantifying preferential flow in soils: a review of different techniques. *J. Hydrol.* 378 (2009), 179–204.
- Bouffard, S.C., 2008. Agglomeration for heap leaching: equipment design, agglomerate quality control, and impact on the heap leach process. *Miner. Eng.* 21, 1115–1125.
- Bowell, R.J., Parshley, J.V., McClelland, G., Upton, B., Zhan, G., 2009. Geochemical evaluation of heap rinsing of the Gold Acres Heap, Cortez joint venture, Nevada. *Miner. Eng.* 22, 477–489.
- Catalan, L.J., Li, M.G., 2000. Decommissioning of copper heap-leach residues by rinsing with water and alkaline solutions—a pilot scale study. *Environ. Eng. Sci.* 17, 191–202.
- Chávez, R.E., Tejero, A., Cifuentes, G., Hernández, E., Aguilar, D., 2015. Imaging fractures beneath a residential complex using novel 3-D electrical resistivity arrays. *J. Environ. Eng. Geophys.* 20, 219–233.
- Cook, S.S., 1994. The Geologic History of Supergene Enrichment in the Porphyry Copper Deposits of Southwestern North America. (Unpublished Ph.D. dissertation). University of Arizona, p. 163.
- Cubbage, B., Rucker, D.F., Zaebst, B., Gillis, J., Cain, J., 2016. Geophysical heap characterization throughout construction and operations of the Carlota Mine. Proceedings of Heap Leach Mining Solutions 2016, October 18–20, 2016, Lima, Peru.
- Dunbar, J., Allen, P., White, J., Neupane, R., Xu, T., Wolfe, J., Arnold, J., 2015. Characterizing a shallow groundwater system beneath irrigated sugarcane with electrical resistivity and radon (^{222}Rn). *J. Environ. Eng. Geophys.* 20, 165–181.
- Ghorbani, Y., Franzidis, J.P., Petersen, J., 2016. Heap leaching technology—current state, innovations, and future directions: a review. *Miner. Process. Extr. Metall. Rev.* 37 (2), 73–119.
- Jarvis, N.J., Villholth, K.G., Ulen, B., 1999. Modelling particle mobilization and leaching in macroporous soil. *Eur. J. Soil Sci.* 50, 621–632.
- Lizama, H.M., Harlamovs, J.R., McKay, D.J., Dai, Z., 2005. Heap leaching kinetics are proportional to the irrigation rate divided by heap height. *Miner. Eng.* 18, 623–630.
- Loke, M.H., Chambers, J.E., Rucker, D.F., Kuras, O., Wilkinson, P.B., 2013. Recent developments in the direct-current geoelectrical imaging method. *J. Appl. Geophys.* 95, 135–156.
- Mahmoudian, A.R., Sadrezaad, S.K., Manafi, Z., 2014. Simulation of bioleaching heat effects for enhancement of copper recovery from sarcheshmeh chalcocopyrite. *Metall. Mater. Trans. B Process Metall. Mater. Process. Sci.* 45, 1204–1212.
- Mellado, M.E., Casanova, M.P., Cisternas, L.A., Gálvez, E.D., 2011. On scalable analytical models for heap leaching. *Comput. Chem. Eng.* 35, 220–225.
- McBride, D., Gebhardt, J.E., Cross, M., 2012. A comprehensive gold oxide heap leach model: development and validation. *Hydrometallurgy* 113–114, 98–108.
- Peterson, N.P., 1962. *Geology and Ore Deposits of the Globe-Miami district, Arizona*. 342. US Government Printing Office.
- Rezanezhad, F., Vogel, H.-J., Roth, K., 2006. Experimental study of fingered flow through initially dry sand. *Hydrol. Earth Syst. Sci. Discuss.* 3, 2595–2620.
- Rucker, D.F., 2010. Moisture estimation within a mine heap: an application of cokriging with assay data and electrical resistivity. *Geophysics* 75 (1), B11–B23.
- Rucker, D.F., 2015. Deep well rinsing of a copper oxide heap. *Hydrometallurgy* 153, 145–153.
- Rucker, D.F., Glaser, D.R., 2015. Standard, random, and optimum array conversions from two-pole resistance data. *J. Environ. Eng. Geophys.* 20, 207–217.
- Rucker, D.F., Schindler, A., Levitt, M.T., Glaser, D.R., 2009. Three-dimensional electrical resistivity imaging of a gold heap. *Hydrometallurgy* 98 (3–4), 267–275.
- Rucker, D.F., Crook, N., Winterton, J., McNeill, M., Baldyga, C.A., Noonan, G., Fink, J.B., 2014. Real-time electrical monitoring of reagent delivery during a subsurface amendment experiment. *Near Surface Geophysics*. 12, pp. 151–163.
- Rucker, D.F., Milzarek, M.A., Baldyga, C.A., Cubbage, B., 2015. Investigating Leaching Alternatives for Heterogeneous Heap Leach Pads. Proceedings of Heap Leach Solutions, 2015. September 14–16, 2015, Reno, USA.
- Saririchi, T., Azad, R.R., Arabian, D., Molaie, A., Nemati, F., 2012. On the optimization of sphalerite bioleaching: the inspection of intermittent irrigation, type of agglomeration, feed formulation and their interactions on the bioleaching of low-grade zinc sulfide ores. *Chem. Eng. J.* 187, 217–221.
- Seal, T., Rucker, D.F., Winterton, J., 2012. Enhancing gold recovery using hydro-jex at Cripple Creek and Victor gold mine CO. In: Young, C.A., Luttrell, G.H. (Eds.), *Separation Technologies for Minerals, Coal & Earth Resources*. Society for Mining, Metallurgy, and Exploration, Denver, CO.
- Seyfried, M.S., Rao, P.S.C., 1987. Solute transport in undisturbed columns of an aggregated tropical soil: preferential flow effects. *Soil Sci. Soc. Am. J.* 51, 1434–1444.
- Silver, R., 2013. *Unsaturated Flow Analysis of Heap Leach Soils* (MS Thesis., Boston College).

- Sinclair, L., Thompson, J., 2015. In situ leaching of copper: Challenges and future prospects. *Hydrometallurgy* 157, 306–324.
- Swarzenski, P.W., Johnson, C.D., Lorenson, T.D., Conaway, C.H., Gibbs, A.E., Erikson, L.H., Richmond, B.M., Waldrop, M.P., 2016. Seasonal electrical resistivity surveys of a coastal bluff, Barter Island, North Slope Alaska. *J. Environ. Eng. Geophys.* 21, 37–42.
- Trujillo, J.Y., Cisternas, L.A., Gálvez, E.D., Mellado, M.E., 2014. Optimal design and planning of heap leaching process. Application to copper oxide leaching. *Chem. Eng. Res. Des.* 92, 308–317.
- Winterton, J., Rucker, D.F., 2013. Optimal Strategies for Leach Pad Injection Operations. Society of Mining Metallurgical and Exploration (SME) Annual Meeting, Phoenix, AZ (February 27–March 2, 2013).
- Wu, A., Yin, S., Liu, J., Yang, B., 2006. Formative mechanism of preferential solution flow during dump leaching. *J. Cent. S. Univ. Technol.* 13, 590–594.